PRAMANA
— journal of
physics

Vol. 81, No. 5
November 2013
pp. 775–790

Coupling constant in dispersive model

R SALEH-MOGHADDAM* and M E ZOMORRODIAN
Department of Physics, Faculty of Physics, Ferdowsi University of Mashhad,
91775-1436, Mashhad, Iran
*Corresponding author. E-mail: R_saleh88@yahoo.com

MS received 23 January 2013; revised 14 July 2013; accepted 18 July 2013
DOI: 10.1007/s12043-013-0608-2; ***e*Publication:** 23 October 2013

Abstract. The average of the moments for event shapes in $e^+e^- \to$ hadrons within the context of next-to-leading order (NLO) perturbative QCD prediction in dispersive model is studied. Moments used in this article are $\langle 1 - T\rangle$, $\langle\rho\rangle$, $\langle B_T\rangle$ and $\langle B_W\rangle$. We extract α_s, the coupling constant in perturbative theory and α_0 in the non-perturbative theory using the dispersive model. By fitting the experimental data, the values of $\alpha_s(M_{Z^0}) = 0.1171 \pm 0.00229$ and $\alpha_0\,(\mu_I = 2\,\text{GeV}) = 0.5068 \pm 0.0440$ are found. Our results are consistent with the above model. Our results are also consistent with those obtained from other experiments at different energies. All these features are explained in this paper.

Keywords. Electron and positron scattering; perturbative calculations; quantum Monte Carlo; strong coupling expansions.

PACS Nos 12.38.Aw; 11.15.Me; 34.80.−i; 12.38.Bx

1. Introduction

The study of hadronic final states in e^+e^- annihilation allows precise tests of the theory of strong interaction and quantum chromodynamics (QCD), using event-shape observables for the analysis of hadronic events. Alternatively, there exist models describing hadronization analytically. These models are: the dispersive model [1], the shape function [2] and the single dressed gluon approximation [3,4]. Our aim is to study dispersive model qualitatively and quantitatively by measuring the strong coupling and the model parameters. The dispersive model is based on the assumption of a non-perturbatively continued strong coupling. Their parameters can be determined (i.e. the value of α_s at some reference energy) and the assumption of universality of these parameters can be probed.

The outline of the paper is as follows: In §2, the observables used in this analysis are presented. Section 3 describes the power correction as well as the perturbative QCD predictions, and introduces analytical models which describe the hadronization process. The simulated data (PYTHIA) for event shape moments are compared by measuring AMY experimental data in §4. Also, a review of the work achieved on this subject in LEP by L3 and DELPHI is made. Finally, §5 gives summary and conclusions.

2. Event-shape variables

When we study observables in the process $e^+e^- \to$ hadrons, it is found that the perturbative QCD predictions have to be complemented by non-perturbative corrections of the form $1/Q^P$, where Q is the centre of mass energy ($E_{\rm cm}$) and the power P depends on the particular observable [5].

Event-shape variables measure geometrical properties of hadronic final states at high-energy particle collisions. They have been studied at e^+e^- collider experiments. Apart from studying the distributions of these observables, we can also study the mean values as well as higher orders for the moments of event-shape variables.

The most common observables y of the three jet type are: thrust, the heavy jet mass, the total and wide jet broadening.

Definitions of these observables are given below [6]:

2.1 *Thrust (T)*

The thrust value of a hadronic event is defined by the expression

$$T = \max\left(\frac{\sum_i |\vec{p}_i \cdot \vec{n}|}{\sum_i |\vec{p}_i|}\right), \tag{1}$$

where $\vec{p}_i$ denotes the three-momentum of particle i and the sum runs over all particles in the final states. The value of $\vec{n}$ for which the maximum is attained is called the thrust axis and denoted by $\vec{n}_{\rm T}$. The value of thrust ranges between 0.5 and 1, where $T = 1$ corresponds to an ideal collinear two-jet event and $T = 0.5$ corresponds to a perfectly spherical event.

Usually one considers the variable $t = 1 - T$ instead of the thrust T, such that the two jet regions correspond to $t \to 0$.

2.2 *Heavy jet mass $M_{\rm H}$*

The plane orthogonal to the thrust axis divides the space into two hemispheres H_1 and H_2. An invariant mass is calculated from the particles in each of the two hemispheres defined by the thrust axis. The hemisphere masses are given as

$$M_i^2 = \left(\sum_{j \in H_i} p_j\right)^2, \ i = 1, 2, \tag{2}$$

where p_j denotes the four-momentum of particle j. The heavy hemisphere mass $M_{\rm H}$ is then defined as

$$M_{\rm H}^2 = \max(M_1^2, M_2^2). \tag{3}$$

The above variable is scaled by the visible energy which, after correction for detector resolution, acceptance and for initial state radiation, equals to

$$\rho = \frac{M_{\rm H}^2}{Q^2}, \tag{4}$$

where Q is the centre of mass energy.

2.3 *Jet broadening B*

The jet broadening is calculated by the expression

$$B_k = \left(\frac{\sum_{i \in H_k} |\vec{p}_i \times \vec{n}_T|}{2 \sum_i |\vec{p}_i|} \right) \tag{5}$$

for each of the two hemispheres (H_k, $k = 1, 2$), defined above. The total jet broadening is given by

$$B_T = B_1 + B_2. \tag{6}$$

The wide jet broadening is defined as

$$B_W = \max(B_1, B_2). \tag{7}$$

The present paper focusses on the distributions of collective variables.

3. Power corrections

The value of α_s can be assessed by the energy dependence of mean values of the event-shape distributions. The mean values of the observables considered in this analysis are calculated up to $\mathcal{O}(\alpha_s^2)$. The DMW model of Dokshitzer, Marchesini and Webber makes the assumption that evolution of α_s to energies below the Landau pole is possible but the form of $\alpha_s(\mu)$ is *a priori* unknown. A non-perturbative parameter α_0 is introduced as the 0th moment over $\alpha_s(\mu)$ [7].

The analytical power ansatz for non-perturbative corrections by Dokshitzer and Webber [8,9] including the Milan factor established by Dokshitzer [10,11] is used to determine α_s from mean event shapes. This ansatz provides an additive term to the perturbative $\mathcal{O}(\alpha_s^2)$ QCD prediction [12].

$$\langle y \rangle = \langle y^{\text{pert}} \rangle + \langle y^{\text{pow}} \rangle = \frac{1}{\sigma_{\text{tot}}} \int y \frac{\mathrm{d}y}{\mathrm{d}\sigma} \mathrm{d}\sigma. \tag{8}$$

For an observable event, the perturbative prediction is

$$\langle y^{\text{pert}} \rangle = \bar{A}_F \left(\frac{\alpha_s(\mu)}{2\pi} \right) + \left(\bar{B}_F + \bar{A}_F \beta_0 \log \left(\frac{\mu^2}{E_{\text{cm}}^2} \right) \right) \left(\frac{\alpha_s(\mu)}{2\pi} \right)^2, \tag{9}$$

where $\bar{A}_F = A_F$, $\bar{B}_F = B_F - \left(\frac{3}{2}\right) C_F A_F$, $\beta_0 = (33 - 2N_F)/12\pi$ and μ is the renormalization scale. The coefficients A_F and B_F were determined from the $\mathcal{O}(\alpha_s^2)$ perturbative calculations [13]. The second term accounts for the difference between the total cross-section used in the measurement and the Born level cross-section used in the perturbative calculation. The numerical values of these coefficients are tabulated in table 1 [13]. QCD colour factors are:

$$C_A = 3, \quad C_F = \frac{N^2 - 1}{2N} = \frac{4}{3} \tag{10}$$

for $N = 3$ colour quarks.

Table 1. Contribution to event-shape moment at LO, NLO [13].

		$\langle(1-T)^n\rangle$	$\langle(\rho)^n\rangle$	$\langle(B_{\mathrm{W}})^n\rangle$	$\langle(B_{\mathrm{T}})^n\rangle$
A_{F}	$n=1$	2.1035	2.1035	4.0674	1.0674
	$n=2$	0.1902	0.1902	0.3369	0.3369
	$n=3$	0.02988	0.02988	0.04755	0.04755
	$n=4$	0.005858	0.005858	0.008311	0.008311
	$n=5$	0.001295	0.001295	0.001630	0.001630
B_{F}	$n=1$	44.999 ± 0.002	23.342 ± 0.002	-9.888 ± 0.006	63.976 ± 0.006
	$n=2$	6.2595 ± 0.0004	3.0899 ± 0.0008	4.5354 ± 0.0005	14.719 ± 0.0001
	$n=3$	1.1284 ± 0.0001	0.4576 ± 0.0002	0.6672 ± 0.0001	2.7646 ± 0.0003
	$n=4$	0.24637 ± 0.00003	0.08363 ± 0.00003	0.10688 ± 0.00002	0.60690 ± 0.00006
	$n=5$	0.06009 ± 0.00001	0.01759 ± 0.00001	0.01865 ± 0.00001	0.14713 ± 0.00002

The power correction is given by

$$\begin{aligned}\langle y^{\mathrm{pow}}\rangle &= a_y \mathcal{P} \\ &= a_y \cdot \frac{4C_{\mathrm{F}}}{\pi^2}\mathcal{M}\frac{\mu_{\mathrm{I}}}{E_{\mathrm{cm}}}\left[\alpha_0(\mu_{\mathrm{I}}) - \alpha_{\mathrm{s}}(\mu_{\mathrm{I}}) - \left(\log\left(\frac{\mu}{\mu_{\mathrm{I}}}\right) + 1 + \frac{k}{4\pi\beta_0}\right)\right. \\ &\qquad \left. \times\, 2\beta_0\alpha_0^2(\mu_{\mathrm{I}})\right], \end{aligned} \tag{11}$$

where α_0 is a non-perturbative parameter accounting for the contributions to the event shape below an infrared matching scale $\mu_{\mathrm{I}} \cong 2$. In the $\overline{\mathrm{MS}}$ renormalization scheme, the constant k has the value $k = \left((67/18) - (\pi^2/6)\right) C_{\mathrm{A}} - (5/9)N_{\mathrm{F}}$, with $N_{\mathrm{F}} = 5$ at the energies studied. The Milan Factor $\mathcal{M}$ is known in two loops $\mathcal{M} = 1.49 \pm 20\%$ [10,14], for flavour number $N_{\mathrm{F}} = 3$ at the relevant low scales [15]. Also, for $\mathcal{M}$ that is called non-inclusive Milan factor, we have [16]:

$$\begin{aligned}\mathcal{M} &= 1 + \frac{3.299C_{\mathrm{A}}}{\beta_0} + 2\frac{-0.862C_{\mathrm{A}} - 0.052N_{\mathrm{F}}}{\beta_0} = 1 + \frac{1.575C_{\mathrm{A}} - 0.104N_{\mathrm{F}}}{\beta_0} \\ &= 1.49 \pm 20\%, \qquad \text{for } N_{\mathrm{F}} = 3 \end{aligned} \tag{12}$$

and coefficient a_y depends on the event-shape observable. That is listed in table 2 [10,17].

Table 2. Coefficient a_y of power correction $\propto 1/Q$ of event-shape variables in the dispersive model.

Event-shape variable	$1-T$	B_{T}	B_{W}	ρ
a_y	2	1	1/2	1

For B_{T} and B_{W} there is further correction to $\mathcal{P}$. It arises from the kinematical mismatch between parton direction and thrust direction which are used to define the hemispheres in the broadening variables. This modification is accounted for by a modification to the power correction. In [18], this modification was computed to NLO for the first moment as

$$\mathcal{P}_{\langle B_{\mathrm{W}}\rangle} = \mathcal{P}\left(\frac{\pi}{\sqrt{8C_{\mathrm{F}}\hat{\alpha}_{\mathrm{s}}(1+(k\hat{\alpha}_{\mathrm{s}}/2\pi))}} + \frac{3}{4} - \frac{\beta_0}{6C_{\mathrm{F}}} + \eta_0\right) \tag{13}$$

$$\mathcal{P}_{\langle B_{\mathrm{T}}\rangle} = \mathcal{P}\left(\frac{\pi}{\sqrt{4C_{\mathrm{F}}\hat{\alpha}_{\mathrm{s}}(1+(k\hat{\alpha}_{\mathrm{s}}/2\pi))}} + \frac{3}{4} - \frac{\beta_0}{3C_{\mathrm{F}}} + \eta_0\right). \tag{14}$$

Here, $\hat{\alpha}_{\mathrm{s}} = \alpha_{\mathrm{s}}(e^{-3/4}Q)$ and $\eta_0 = -0.6137$.

In the first approximation, non-perturbative corrections generate a simple shift of the perturbative differential distribution $\mathrm{d}\sigma_{\mathrm{NLO}}/\mathrm{d}y$ of the event-shape variables $1-T$, B_{T}, B_{W} and ρ, when relating parton to hadron level,

$$\frac{\mathrm{d}\sigma_{\mathrm{had}}}{\mathrm{d}y} = \frac{\mathrm{d}\sigma_{\mathrm{NLO}}}{\mathrm{d}y}\left(y - a_y\mathcal{P}\right). \tag{15}$$

This prediction is valid if the value of the event-shape variable y is not too large ($y \ll 1$) and the centre of mass energy Q not too small ($Q \gg (\Lambda_{\mathrm{QCD}}/y)$). The nth moment of an event-shape observable y is defined as

$$\langle y^n\rangle = \int_0^{y_{\max}} y^n \frac{1}{\sigma_{\mathrm{had}}}\frac{\mathrm{d}\sigma}{\mathrm{d}y}\mathrm{d}y, \tag{16}$$

where $y_{\max}$ is the kinematically allowed upper limit of the observable [19].

By inserting (15) in eq. (16) of the moment of order n and naively neglecting the integration over the unphysical range of negative variable values, we obtain

$$\begin{aligned}\langle y^n\rangle &= \int_0^{y_{\max}} y^n \frac{1}{\sigma_{\mathrm{had}}}\frac{\mathrm{d}\sigma}{\mathrm{d}y}\mathrm{d}y = \int_{-a_y\mathcal{P}}^{y_{\max}-a_y\mathcal{P}} (y+a_y\mathcal{P})^n \frac{1}{\sigma_{\mathrm{had}}}\frac{\mathrm{d}\sigma_{\mathrm{pt}}}{\mathrm{d}y}\mathrm{d}y \\ &\approx \int_0^{y_{\max}} (y+a_y\mathcal{P})^n \frac{1}{\sigma_{\mathrm{had}}}\frac{\mathrm{d}\sigma_{\mathrm{pt}}}{\mathrm{d}y}\mathrm{d}y.\end{aligned} \tag{17}$$

Discarding the integration over the kinematically forbidden values of y leads to non-perturbative predictions. The prediction for the moment on hadron level will be [20]

$$\langle y^1\rangle = \langle y^1\rangle_{\mathrm{NLO}} + a_y\mathcal{P} \tag{18}$$

$$\langle y^2\rangle = \langle y^2\rangle_{\mathrm{NLO}} + 2\langle y^1\rangle_{\mathrm{NLO}}\cdot a_y\mathcal{P} + (a_y\mathcal{P})^2 \tag{19}$$

$$\langle y^3\rangle = \langle y^3\rangle_{\rm NLO} + 3\langle y^2\rangle_{\rm NLO}\cdot a_y\mathcal{P} + +3\langle y^1\rangle_{\rm NLO}\cdot (a_y\mathcal{P})^2 + (a_y\mathcal{P})^3 \quad (20)$$

$$\langle y^4\rangle = \langle y^4\rangle_{\rm NLO}+4\langle y^3\rangle_{\rm NLO}\cdot a_y\mathcal{P}+6\langle y^2\rangle_{\rm NLO}\cdot (a_y\mathcal{P})^2+4\langle y^1\rangle_{\rm NLO}\cdot (a_y\mathcal{P})^3 + (a_y\mathcal{P})^4 \quad (21)$$

$$\langle y^5\rangle = \langle y^5\rangle_{\rm NLO}+5\langle y^4\rangle_{\rm NLO}\cdot a_y\mathcal{P}+10\langle y^3\rangle_{\rm NLO}\cdot (a_y\mathcal{P})^2+10\langle y^2\rangle_{\rm NLO}\cdot (a_y\mathcal{P})^3 + 5\langle y^1\rangle_{\rm NLO}\cdot (a_y\mathcal{P})^4 + (a_y\mathcal{P})^5. \quad (22)$$

The dispersive model gives predictions for several observables and contains only universal free parameters $\alpha_s(M_{Z^0})$ and $\alpha_0(\mu_I)$.

4. Physics results

In this section, we use the event-shape variables mentioned above, for calculating both the strong coupling constant $\alpha_s(M_{Z^0})$ and the non-perturbative coupling parameter $\alpha_0(\mu_I = 2\ \text{GeV})$. To achieve this, we do our analysis up to the fifth order of power corrections.

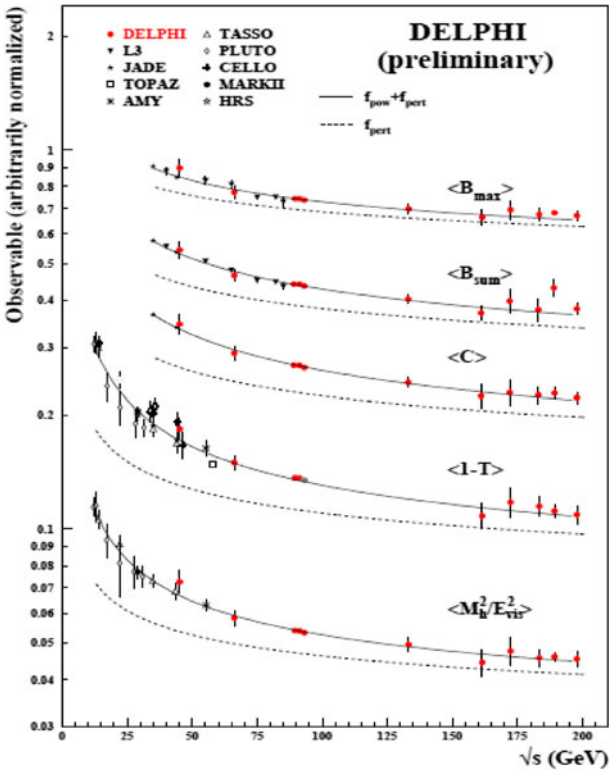

Figure 1. First moments of event shapes from DELPHI [7].

We explain first the work performed on the above subject by other experiments. Figure 1 presents the DELPHI high-energy data together with the data obtained from other experiments [7]. The fit of $\mathcal{O}(\alpha_s^2)$ perturbative QCD prediction combined with a power correction describes the data well. All diagrams show that by increasing energy, the amount of these variables will tend to zero. However, they do not vanish, because some hadrons have a finite transverse momentum (P_T).

Figure 2 shows the results by L3 for second moments from the analysis of the LEP high-energy data as well as from the low-energy data obtained by selecting events at $\sqrt{S} = M_{Z^0}$ with hard initial or final-state photon radiation [7].

Using the above results and fitting the corresponding distributions from the analyses of the DMW power correction model, table 3 and also figure 3 show the values for α_s and α_0 extracted from their data.

In order to clarify the situation further, we extend this analysis by using the events obtained by the AMY (the range of energy between 52 and 60 GeV) at KEK, as well as

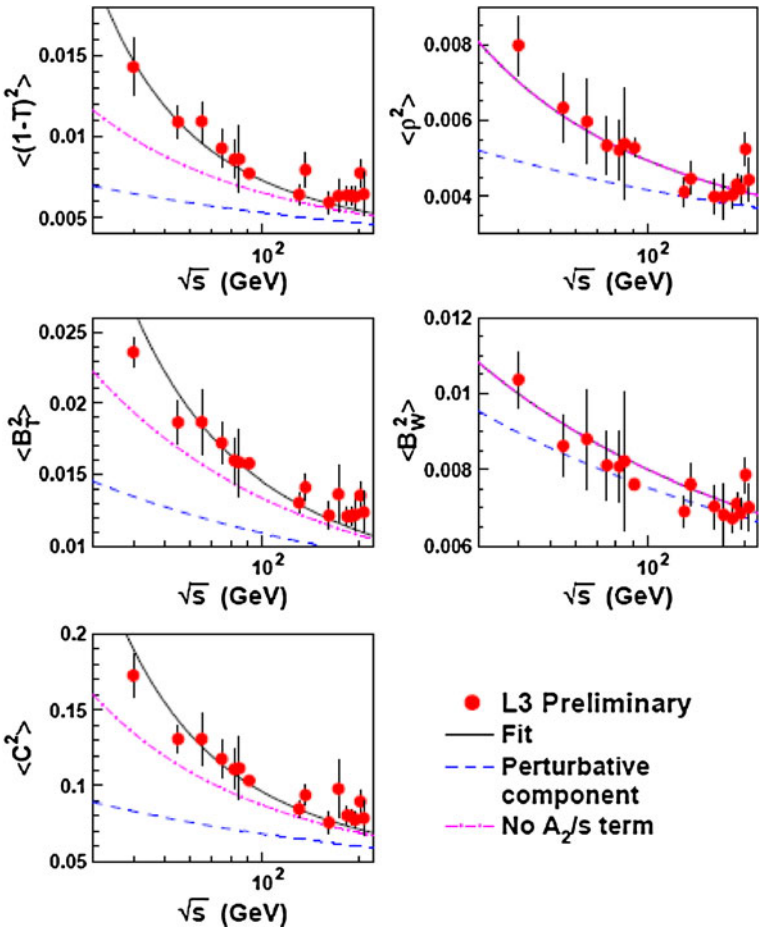

Figure 2. The second moments of the event shapes from L3 [7,21].

Table 3. The values of $\alpha_s(M_{Z^0})$ and α_0 (2 GeV) [22].

	Exp. $\sqrt{s}$ range (GeV)	ALEPH 12(35)–206	DELPHI 12–202	L3 41–206	MPI 12(35)–189
$1-T$	$\alpha_s(M_{Z^0})$	0.1207 ± 0.0019	0.1241 ± 0.0034	0.1164 ± 0.0060	0.1217 ± 0.0060
	α_0 (2 GeV)	0.539 ± 0.011	0.491 ± 0.018	0.518 ± 0.059	0.528 ± 0.064
	χ^2/d.o.f.	69/43	27/41	18/14	50/41
M_H, ρ	$\alpha_s(M_{Z^0})$	0.1161 ± 0.0018	0.1197 ± 0.0122	0.1051 ± 0.0051	0.1165 ± 0.0043
	α_0 (2 GeV)	0.627 ± 0.020	0.339 ± 0.263	0.421 ± 0.037	0.663 ± 0.095
	χ^2/d.o.f.	50/40	10/15	13/14	24/35
B_T	$\alpha_s(M_{Z^0})$	0.1148 ± 0.0025	0.1174 ± 0.0029	0.1163 ± 0.0042	0.1205 ± 0.0049
	α_0 (2 GeV)	0.492 ± 0.020	0.463 ± 0.033	0.449 ± 0.054	0.445 ± 0.054
	χ^2/d.o.f.	7/18	9/23	9/14	24/28
B_W	$\alpha_s(M_{Z^0})$	0.1179 ± 0.0028	0.1167 ± 0.0019	0.1169 ± 0.0042	0.1178 ± 0.0025
	α_0 (2 GeV)	0.467 ± 0.037	0.438 ± 0.049	0.342 ± 0.079	0.425 ± 0.097
	χ^2/d.o.f.	11/18	10/23	14/14	10/29
C	$\alpha_s(M_{Z^0})$	0.1228 ± 0.0027	0.1222 ± 0.0036	0.1164 ± 0.0047	0.1218 ± 0.0059
	α_0 (2 GeV)	0.461 ± 0.016	0.444 ± 0.022	0.457 ± 0.040	0.461 ± 0.048
	χ^2/d.o.f.	17/18	12/23	12/14	18/26
D	$\alpha_s(M_{Z^0})$			0.1046 ± 0.0124	
	α_0 (2 GeV)	–	–	0.682 ± 0.096	–
	χ^2/d.o.f.			24/14	

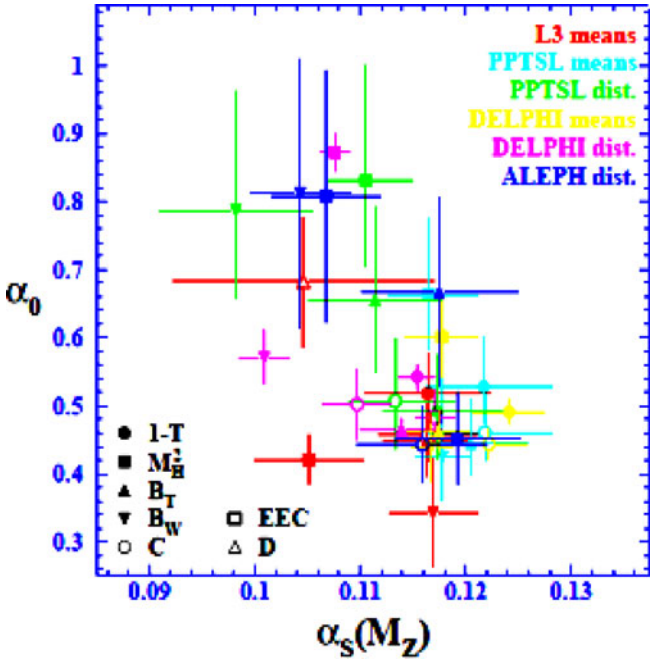

Figure 3. Measurements of $\alpha_s(M_{Z^0})$ and α_0 (2 GeV) from different experiments such as: ALEPH, DELPHI, L3 and MPI [22].

the simulated events (PYTHIA) up to the fifth order. The reason behind this is to see if there are any differences between the lower- and the higher-order moments.

In figure 4 we show the mean value of $\langle 1 - T \rangle$ up to the fifth order as a function of the centre-of-mass energy fitted to the dispersive prediction. As the results obtained

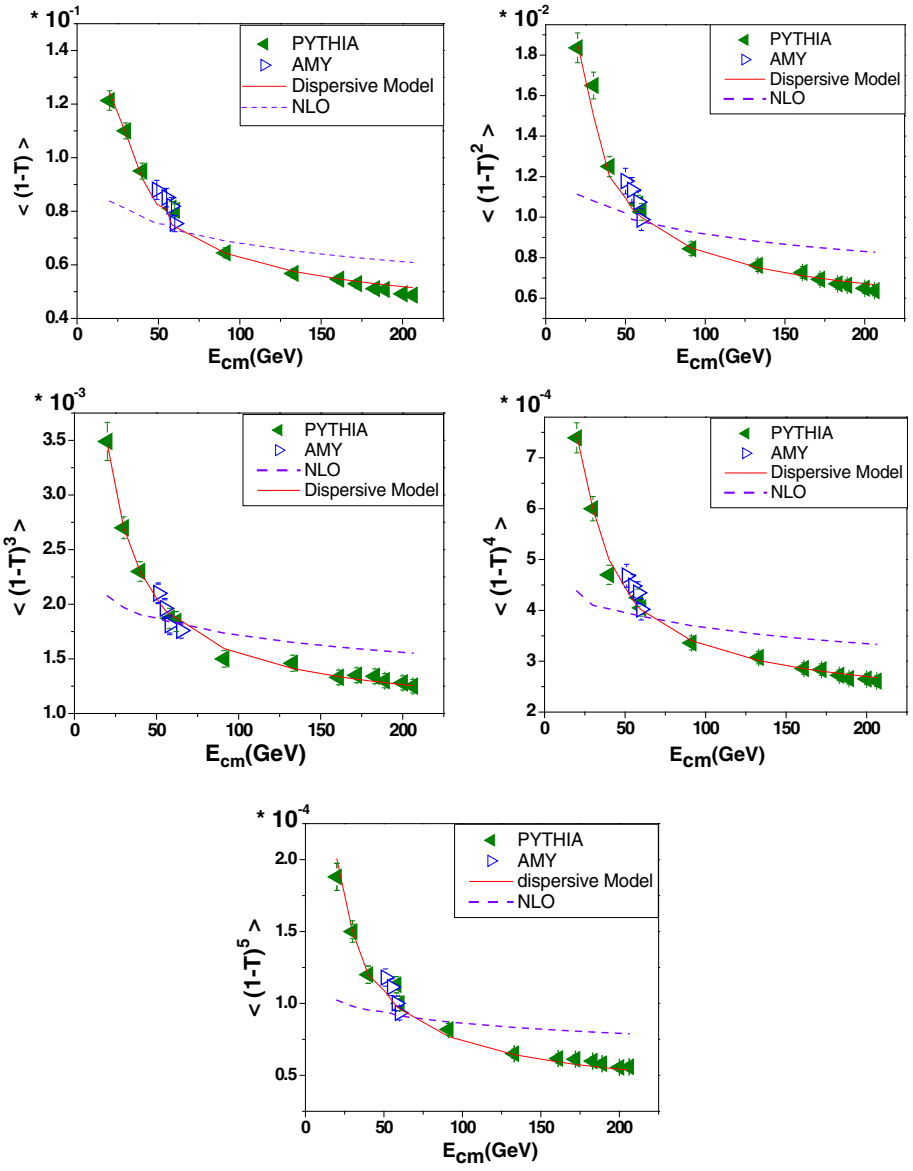

Figure 4. Fits of the dispersive prediction to PYTHIA and AMY measurements of 1−thrust moments. The solid line shows the prediction with fitted values of $\alpha_s(M_{Z^0})$ and $\alpha_0(\mu_I)$.

by the AMY data coincide with those obtained from the MC, we have made a single fitting procedure to both data. We observe that results for the dispersive model follow the same trend as those for the Monte Carlo data. In addition, the values for the AMY in the range of 52–60 GeV are consistent with both the Monte Carlo and the dispersive model.

We include on all figures the fitted distribution obtained from the NLO predictions. We observe that the distributions for the dispersive model (solid line) are in good agreement with those for the Monte Carlo when compared with the NLO prediction because the NLO does not include the power correction. For comparison, we show in figure 5 the results by the JADE and OPAL experiments up to fifth order [15].

We do a similar analysis for B_W, B_T and ρ in figures 6, 7 and 8 respectively. Due to the similarity between the distributions, we have deliberately omitted the distributions of the

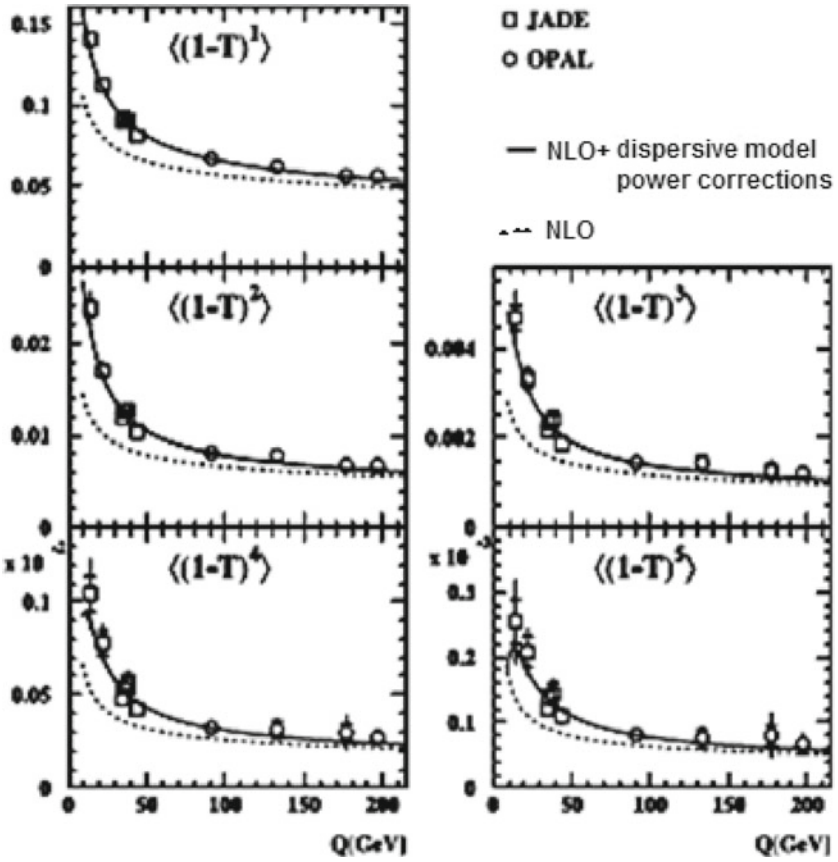

Figure 5. The dispersive prediction to JADE and OPAL measurements of 1−thrust moments. The solid line shows the prediction with fitted values of $\alpha_s(M_{Z^0})$ and $\alpha_0(\mu_I)$ [15].

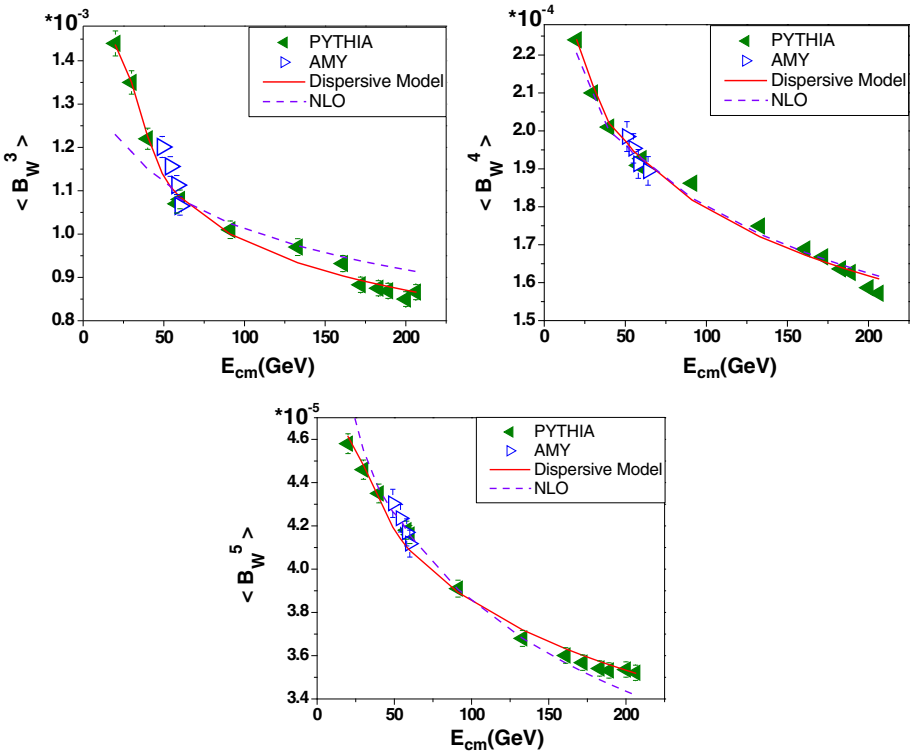

Figure 6. Fits to distributions of the wide jet broadening (B_{W}) for different centre-of-mass energies.

first two moments. For higher moments ($n \geq 2$) of the jet broadening B_{T} and B_{W} the kinematical modifications to the power correction are not known at present. If we do not apply these corrections to the higher moments, the mutual consistency of the parameter extractions from different moments of B_{T} deteriorates considerably, while minor improvements in consistency are observed on B_{W} [19].

Mass effects, in particular on ρ moments, have not been considered in obtaining the averages for α_{s} and α_0. However, Salam and Wicke [23] showed that mass effects are smaller than effects due to the non-inclusiveness of the heavy jet mass, used in this analysis.

In a second step, we achieve α_{s} and α_0 measurements obtained from different event-shape variables. Figures 9 and 10 show our results for $\alpha_{\mathrm{s}}(M_{Z^0})$ and $\alpha_0\,(\mu_{\mathrm{I}} = 2\ \mathrm{GeV})$ respectively.

Figure 9 indicates that the values of $\alpha_{\mathrm{s}}(M_{Z^0})$ measured from $\langle 1 - T \rangle$, $\langle \rho \rangle$, $\langle B_{\mathrm{W}} \rangle$ and $\langle B_{\mathrm{T}} \rangle$ are in agreement within errors with previous analysis [15] and references in it. In particular the $\alpha_{\mathrm{s}}(M_{Z^0})$ values are steeply rising with moment order for the variables $\langle (1 - T)^n \rangle$, $\langle \rho^n \rangle$ and $\langle (B_{\mathrm{T}})^n \rangle$. On the other hand, the value of $\alpha_{\mathrm{s}}(M_{Z^0})$ for $\langle (B_{\mathrm{W}})^n \rangle$ decreases when order n increases, because these moments are not universal [15]. Our

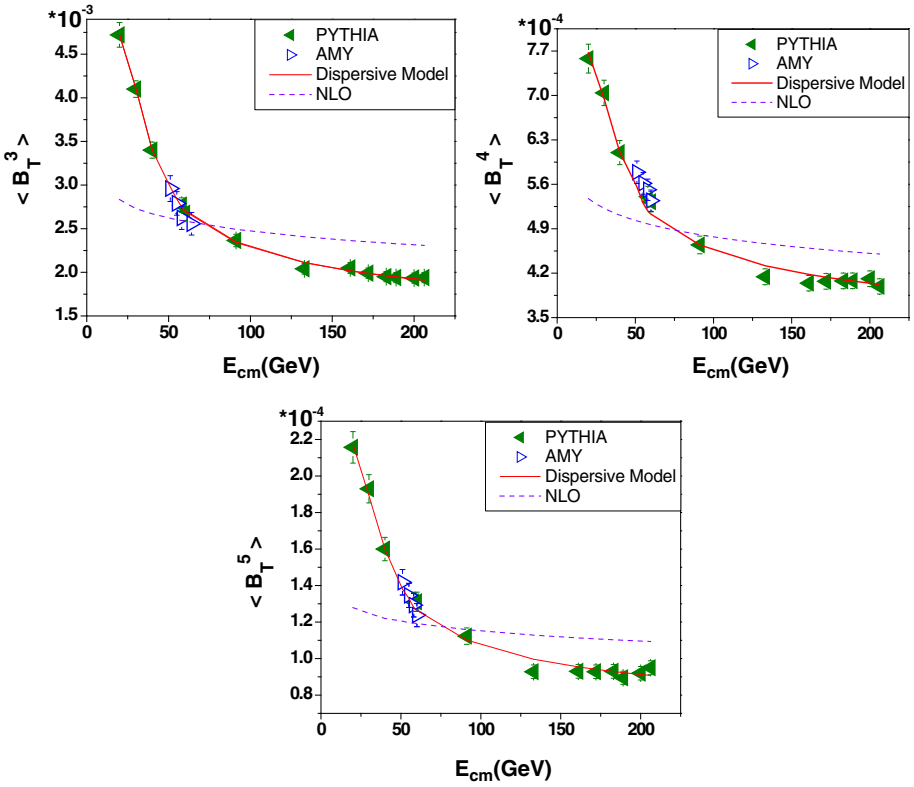

Figure 7. Fits to distributions of the total jet broadening (B_T) for different centre-of-mass energies.

results are consistent with the values obtained from JADE and OPAL experiments as we can see in figure 11.

The values of α_0 ($\mu_I = 2$ GeV) for four moments of event-shape observables in figure 10 show slow increase with increasing order n.

The $\alpha_0(\mu_I)$ values of B_W are much lower than those of the other observables. Fit to PYTHIA and the AMY data of $\langle B_W^1 \rangle$ gives $\alpha_s(M_{Z^0}) = 0.12382 \pm 0.0022$ and α_0 ($\mu_I = 2$ GeV) $= 0.3112 \pm 0.08$ GeV. So, at lower energies where the coupling is large, the compensation is stronger, and the power correction for this parameter is not universal; while different orders for B_T show very steep rising, because it is both a universal and a complete variable.

Finally, the combined results for α_s and α_0 values in event-shape moments are summarized in table 4. In this table, we observe that the error in different orders of event shapes on extraction of $\alpha_s(M_{Z^0})$ from B_W is considerably smaller than those of ρ, $1 - T$ and B_T. Consequently, the theoretical description of the moments of B_W displays a higher perturbative stability, which is reflected in the theoretical uncertainty on $\alpha_s(M_{Z^0})$ derived from them. We conclude that our results obtained from PYTHIA and the AMY data are

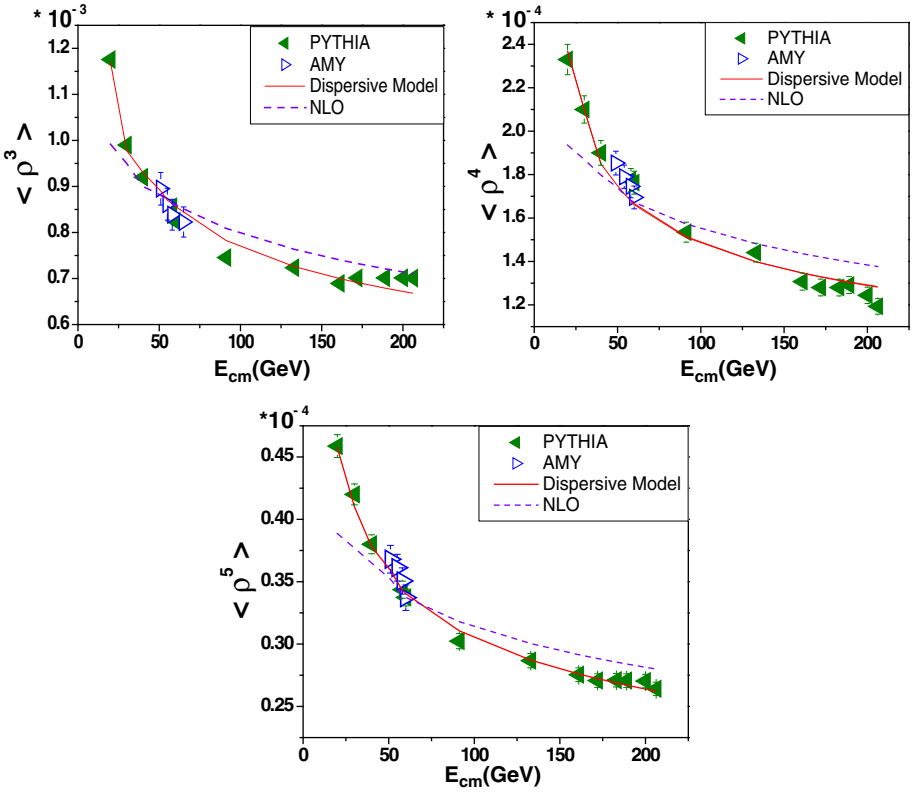

Figure 8. Fits to distributions of the heavy jet mass (ρ) for different centre-of-mass energies.

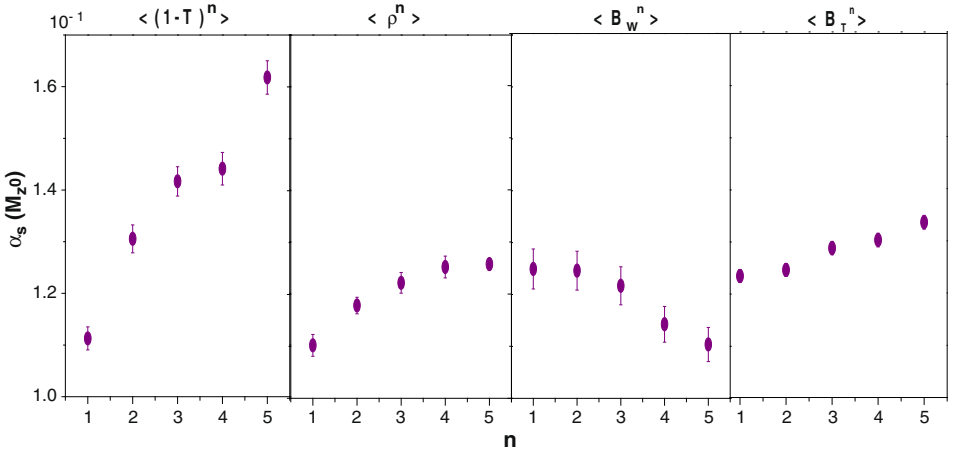

Figure 9. Measurement of $\alpha_s(M_{Z^0})$ using moments of four event-shape observables.

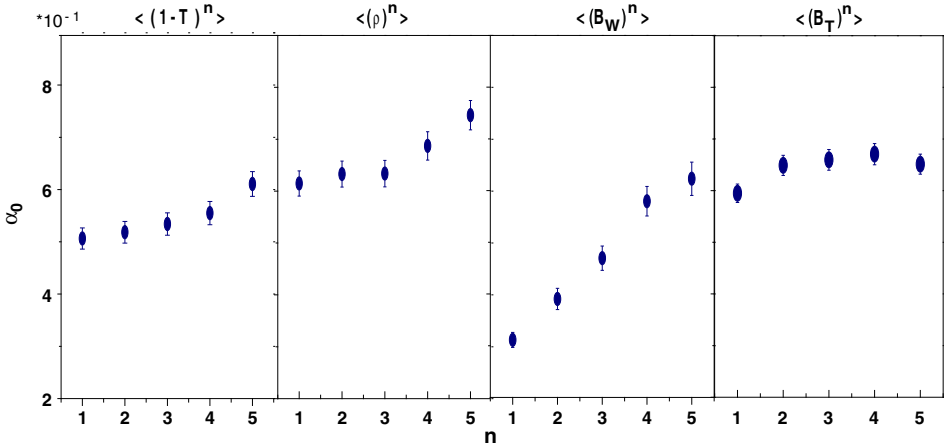

Figure 10. Measurement of $\alpha_0\,(2\,\mathrm{GeV})$ using moments of four event-shape observables.

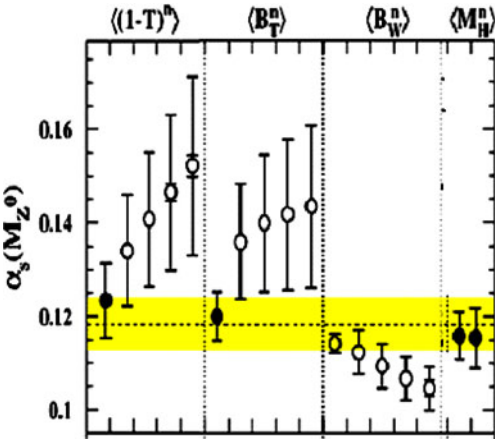

Figure 11. Measurements of $\alpha_s(M_{Z^0})$ and $\alpha_0\,(\mu_I = 2\,\mathrm{GeV})$ from moments of four event-shape variables at PETRA and LEP energies [15].

consistent with those obtained from LEP (table 3, figure 3) and also with those obtained from JADE experiment (figure 11).

5. Conclusions

In this paper, we studied the perturbative and non-perturbative contributions to the moments of event shapes in e^+e^- annihilation. We introduced an analytical hadronization model called dispersive model. We extended this model for non-perturbative power corrections to include all logarithmic corrections to NLO order.

Table 4. α_s and α_0 values up to the fifth order for combined Monte Carlo and the AMY data.

Event-shape variables	n	$\alpha_s(M_{Z^0})$	α_0 ($\mu_I = 2\,\text{GeV}$)
$\langle(1-T)^n\rangle$	1	0.11128 ± 0.00299	0.50639 ± 0.02593
	2	0.13055 ± 0.00168	0.51834 ± 0.01019
	3	0.14167 ± 0.00166	0.53409 ± 0.00798
	4	0.14412 ± 0.00134	0.55495 ± 0.0088
	5	0.16179 ± 0.01171	0.61062 ± 0.07696
$\langle(\rho)^n\rangle$	1	0.1102 ± 0.00246	0.6147 ± 0.0327
	2	0.11788 ± 0.00044	0.63289 ± 0.00486
	3	0.1225 ± 0.0014	0.63373 ± 0.01324
	4	0.1253 ± 0.0021	0.68711 ± 0.01544
	5	0.12585 ± 0.00067	0.7464 ± 0.00726
$\langle(B_W)^n\rangle$	1	0.12382 ± 0.00229	0.31126 ± 0.08593
	2	0.1245 ± 0.00017	0.3904 ± 0.00057
	3	0.12159 ± 0.00065	0.4693 ± 0.02022
	4	0.11421 ± 0.00069	0.57942 ± 0.03309
	5	0.11033 ± 0.00053	0.62981 ± 0.02799
$\langle(B_T)^n\rangle$	1	0.12326 ± 0.00243	0.59486 ± 0.03171
	2	0.12442 ± 0.00072	0.64896 ± 0.01384
	3	0.12961 ± 0.00074	0.65861 ± 0.01302
	4	0.13015 ± 0.00114	0.67062 ± 0.02031
	5	0.13356 ± 0.0014	0.65128 ± 0.0256

We used this newly obtained theoretical description of the event-shape moments to analyse data from AMY and PYTHIA for determining the strong coupling constant α_s and the non-perturbative parameter α_0. We also reviewed the results obtained from LEP (DELPHI and L3) and also the results obtained from JADE experiments. The most common variables used are: thrust, heavy jet mass, wide jet broadening and total jet broadening.

We have done it by fitting the experimental data with this model. We observed that results obtained from the dispersive model follow the same trend as those of the Monte Carlo data. In addition, the value for the AMY data at the range of 52–60 GeV centre-of-mass energy is consistent with both the Monte Carlo distribution and the dispersive model.

In this fitting, we extracted the coupling constant $\alpha_s(M_{Z^0})$ and also the non-perturbative parameter $\alpha_0(\mu_I)$ in low-energy momentum scale.

Our best fitting result with dispersive model for the values of average coupling constant are: $\alpha_s(M_{Z^0}) = 0.1171 \pm 0.00229$ and $\alpha_0\,(\mu_I = 2\text{ GeV}) = 0.5068 \pm 0.0440$ GeV. Our results are consistent with those obtained from both LEP and JADE experimental values for these parameters.

References

[1] Y Dokshitzer, G Marchesini and B Webber, *Nucl. Phys. B* **469**, 93 (1996)
[2] G Korchemsky and S Tafat, *J. High Energy Phys.* **0010**, 010 (2000)
[3] E Gardi and G Grunberg, *J. High Energy Phys.* **9911**, 016 (1999)
[4] E Gardi, *J. High Energy Phys.* **0004**, 030 (2000)
[5] G Dissertori, arXiv:hep-ex/9904033v1 (1999)
[6] P A Movilla Fernandez, O Biebel, S Bethke and S Kluth, arXiv:hep-ex/9708034 v2 (1997)
[7] S Kluth, *Nucl. Phys. B, Proc. Suppl.* **96**, 54 (2001)
[8] Y L Dokshitzer and B R Webber, *Phys. Lett. B* **352**, 451 (1995)
[9] B R Webber, Talk given at the workshop on DIS and QCD in Paris, arXiv:hep-ph/9510283 (1995)
[10] Yu L Dokshitzer, A Lucenti, G Marchesini and G P Salam, *Nucl. Phys. B* **511**, 396 (1998)
[11] Yu L Dokshitzer, A Lucenti, G Marchesini and G P Salam, arXiv:hep-ph/9802381 (1998)
[12] J Drees, U Flagmeyer, K Hamacher, O Passon, R Reinhardt and D Wicke, *DELPHI Collaboration* 99-19 CONF 219 (1999)
[13] A Gehrmann-De Ridder, T Gehrmann, E W N Glover and G Heinrich, *J. High Energy Phys.* **05**, 106 (2009)
[14] M Dasgupta, L Magnea and G Smye, *J. High Energy Phys.* **11**, 025 (1999)
[15] C Pahl, S Bethke, O Biebel, S Kluth and J Schieck, *Eur. Phys. J. C* **64**, 53 (2009), arXiv:hep-ex/0904 0786 (2009)
[16] Yu L Dokshitzer, arXiv:hep-ph/9911299v2 (1999)
[17] Y Dokshitzer, A Lucenti, G Marchesini and G Salam, *J. High Energy Phys.* **05**, 003 (1998)
[18] O Biebel, *Phys. Rep.* **340**, 165 (2001)
[19] T Gehrmann, M Jaquier and G Luisoni, *Eur. Phys. J. C* **67**, 57 (2010)
[20] S Kluth, Max-Plank-Institute for Physics (Germany), arXiv:hep-ex/0505026v1 (2005)
[21] The L3 Collaboration, *Phys. Lett. B* **489**, 65 (2000), arXiv:hep-ex/0005045v1
[22] S Kluth, Max-Planck-Institute for Physics (Germany), arXiv:hep-ex/0606046v1 (2006)
[23] G Salam and D Wicke, *J. High Energy Phys.* **05**, 061 (2001)